Chapter 12
Rayleigh Waves in the Cosserat Half-Space (Reduced Model) and Half-Space of Damaged Material

Vladimir Erofeev, Artem Antonov, Anna Leonteva, and Alexey Malkhanov

Abstract The peculiarities of propagation of Rayleigh surface waves along the free boundary of the half-space of the Cosserat medium (reduced model), as well as along the free boundary of the half-space made of damaged material, are studied. It is shown that, in contrast to the classical Rayleigh surface wave, a wave propagating along the boundary of the Cosserat half-space has dispersion. In the plane "phase velocity – frequency" for such waves, there are two dispersion branches: lower ("acoustic") and upper ("optical"). As the frequency increases, the phase velocity of the wave related to the lower dispersion branch decreases. The phase velocity of the wave belonging to the upper dispersion branch increases with increasing frequency. The phase velocity of the surface wave in the entire frequency range exceeds the phase velocity of the bulk shear wave. The stresses and displacements arising in the zone of propagation of a surface wave are calculated.

For an isotropic elastic half-space with damage of its material, a self-consistent problem is formulated that includes the dynamic equation of elasticity theory and the kinetic equation of damage accumulation in the material of the medium. This system of equations with boundary conditions expressing the absence of stresses at the boundary of the half-space reduces to a complex dispersion equation. A surface wave propagating along the boundary of a damaged half-space decays in the direction of propagation, and low-frequency perturbations have frequency-dependent dissipation and dispersion. It is shown that the dispersion has an anomalous character. It has been established that with a decrease in the value of the damage factor, in the region of high frequencies, the value of the phase velocity increases, and the group velocity decreases. At very low frequencies, both velocities increase as the damage factor decreases.

Vladimir Erofeev · Artem Antonov · Anna Leonteva · Alexey Malkhanov
Mechanical Engineering Research Institute of Russian Academy of Sciences, 85 Belinskogo str., Nizhny Novgorod 603024, Russian Federation,
e-mail: erof.vi@yandex.ru, artem.antonov@autorambler.ru, aleonav@mail.ru, alexey.malkhanov@gmail.com

H. Altenbach et al. (eds.), *Sixty Shades of Generalized Continua*,
Advanced Structured Materials 170, https://doi.org/10.1007/978-3-031-26186-2_12

Key words: Cosserat half-space · Damaged material · Rayleigh waves · Dispersion · Attenuation

12.1 Introduction

In 1885, Lord Rayleigh (John William Strett) theoretically demostrated that along the plane boundary of a solid elastic half-space with a vacuum or a sufficiently rarefied medium (for example, with air), waves can propagate, the amplitude of which rapidly decreases with depth [1]. These waves, called Rayleigh surface waves, depending on the frequency range, have different applied directions.

Almost immediately it became obvious that Rayleigh waves in the low frequency range (1–100 Hz) are the main type of waves observed during earthquakes. Therefore, they have been studied in detail in seismology for nearly 140 years [2].

The main regularities of the propagation of Rayleigh waves are as follows: the absence of dispersion, i.e. the speed of the wave does not depend on its frequency and is constant for each material; this speed reaches 0.87–0.96 of the speed of the bulk shear wave; the displacement vector has longitudinal and transverse components, while the transverse component always exceeds the longitudinal one.

In the cycle of works by Krylov [3]-[9], awarded by the Acoustics Institute of Great Britain the Rayleigh Medal (often called the Nobel Prize in Acoustics) in 2000, dedicated to the study of elastic earth vibrations generated by trains and motor vehicles, a very high level of earth vibrations generated by high-speed railways was theoretically predicted. These vibrations are generated by high-speed trains moving at a speed higher than the speed of Rayleigh surface waves in the ground. Krylov's theory was experimentally confirmed in 1997–1998 (with his direct participation) on a new high-speed line in Sweden (Gothenburg-Malmo), where on some sections of the route the Rayleigh wave speed was only 45 m/s, and the train speed of 160 km/h was enough to observe the effect. The discovered effect began to be called "ground vibration shock" (by analogy with the well-known sonic boom from a supersonic aircraft), and the generation sources began to be called "trans-Rayleigh trains" [10].

It should be noted that the existence of critical speeds of movement of loads along rail guides, when exceeded, bending waves are generated in the guides, was discussed in the first half of the 1980s in the works of Vesnitsky and his school [11], as well as in the works of G.G. Denisov, V.V. Novikov and E.K. Kugusheva [12]. However, the calculated critical speeds showed the practical unattainability of the effect of generation of bending waves by the vehicle in the guides. It turned out to be easier for the load to overcome the speed of the Rayleigh wave in the soil located under the guide rail, and the guide itself, along with the system of sleepers and ballast, acted as an intermediary between the source of wave generation and the medium in which these waves arose.

At present, the problems of the stability of the movement of high-speed objects along rail guides, the problems of generating bending and bending-torsional waves in rail guides are recognized as relevant and their results serve as methodological

and computational support in setting up experiments on high-speed acceleration of the payload on rocket tracks [13]-[15].

Since the 1950s, Rayleigh waves in the ultrasonic range (frequencies of the order of 10^6 Hz) have been widely used. The state of the surface layer of a sample can be controlled by their assistance (detection of surface and near-surface defects in samples made of metal, glass, plastic and other materials – ultrasonic surface defectoscopy). The influence of the properties of the surface layer of the sample on the velocity and damping of Rayleigh waves makes it possible to use the latter to determine the residual stresses of the surface layer of the metal, the thermal and mechanical properties of the surface layer of the sample [16].

Since the early 1970s, Rayleigh waves with frequencies of 10^7–10^{10} Hz have been widely used in miniature solid-state information processing devices (ultrasonic delay lines, bandpass filters, signal couplers, phase shifters, etc.). At the junction of ultra- and hypersonic acoustics, on the one hand, and solid-state electronics, on the other hand, a branch of knowledge called acoustoelectronics has emerged. Such an important industry as microelectronics based on SAW (i.e., on surface acoustic waves) is based on the principles of acoustoelectronics [17].

Along with the classical continuum model, generalized continuum models are widely used in the mechanics of a deformable solid body [18]-[39]. The most well-known generalized (nonclassical) continuums include the micropolar Cosserat medium and the gradient elastic medium. When working with a micropolar medium, one should distinguish between the general model of a continuum proposed by the brothers Eugène and François Cosserat in 1909, each point of which has three translational and three rotational degrees of freedom [40], its particular case – a model of a micropolar medium with constrained rotation of particles [41], and a reduced model of a micropolar medium, proposed by L. Schwartz, D. Johnson and S. Feng in 1984 [42]-[45]. The model of a gradient elastic medium also appeared at the beginning of the 20th century and is associated with the names of Leroux (1911, 1913) [46, 47] and Jaramillo (1929) [48]. A number of authors have studied Rayleigh surface waves within the framework of the Cosserat continuum [49] and gradient elastic medium [50] models. Below we study the main regularities of Rayleigh wave propagation along the free boundary of the half-space of the Cosserat medium (reduced model), as well as along the free boundary of the half-space made of damaged material (another version of the generalized continuum model).

12.2 Rayleigh Waves in the Cosserat Half-space (Reduced Model)

Let us consider the problem of propagation of elastic surface wave in a reduced dynamic model of the Cosserat medium, which take place in the intermediate state between the classical dynamics theory and the actual model of the Cosserat medium, which has an asymmetry of the stress tensor and the presence of load moments, are considered. In contrast to the latter, in the simplified model, the three of six elasticity

constants are supposed to be equal to zero and, as a result, there is no couple-stress tensor.

The equations of the dynamics of the Cosserat continuum have the form [41]:

$$\begin{aligned} \rho\frac{\partial^2 \boldsymbol{u}}{\partial t^2} - (\lambda+2\mu)\,\mathrm{grad}\,\mathrm{div}\,\boldsymbol{u} + (\mu+\alpha)\,\mathrm{rot}\,\mathrm{rot}\,\boldsymbol{u} - 2\alpha\,\mathrm{rot}\,\boldsymbol{\theta} = 0, \\ I\frac{\partial^2 \boldsymbol{\theta}}{\partial t^2} - (\beta+2\gamma)\,\mathrm{grad}\,\mathrm{div}\,\boldsymbol{\theta} + (\gamma+\varepsilon)\,\mathrm{rot}\,\mathrm{rot}\,\boldsymbol{\theta} - 2\alpha\,\mathrm{rot}\,\boldsymbol{\theta} + 4\alpha\boldsymbol{\theta} = 0. \end{aligned} \tag{12.1}$$

Here $\boldsymbol{u}$ – displacements vector; $\boldsymbol{\theta}$ – rotation vector; ρ – density of the medium, I – a constant characterizing the inertial properties of macrovolume, equal to the product of the moment of inertia of a particle of a substance around any axis passing through its center of gravity by the number of particles per unit volume; λ, μ – Lame constants, $\alpha, \beta, \gamma, \varepsilon$ – new elastic constants of micropolar material satisfying the constraints [41]:

$$\alpha \geq 0,\ \gamma+\varepsilon \geq 0,\ 3\beta+2\gamma \geq 0,\ -(\gamma+\varepsilon) \geq \gamma-\varepsilon \geq (\gamma+\varepsilon)\,. \tag{12.2}$$

In [49] the following dependence was found between these elastic constants:

$$\mu\,(2\gamma+\beta) = (\alpha+\mu)\,(\gamma+\varepsilon)\,. \tag{12.3}$$

Along with the general case, a simplified version of the micropolar medium (Cosserat pseudo-continuum) is also considered, in which a rigid dependence of the rotation vector on the displacement rotor, which coincides with the relations of the classical theory of elasticity, is assumed ($\boldsymbol{\theta} = \frac{1}{2}\,\mathrm{rot}\,\boldsymbol{u}$ – cramped rotation), but at the same time, the moment stresses and asymmetry of the stress tensor are preserved. In such a medium, the symmetric part of the stress tensor depends on the symmetric strain tensor in the same way as in the classical theory of elasticity.

The equations of dynamics of the Cosserat pseudo-continuum have the form [41]:

$$\rho\ddot{\boldsymbol{u}} - (\lambda+\mu)\,\mathrm{grad}\,\mathrm{div}\,\boldsymbol{u} - \mu\Delta\boldsymbol{u} - \frac{1}{4}\,(\gamma+\varepsilon)\,\mathrm{rot}\,\mathrm{rot}\,\Delta\boldsymbol{u} + \frac{1}{4}\,\mathrm{rot}\,\mathrm{rot}\,\ddot{\boldsymbol{u}} = 0. \tag{12.4}$$

In addition to this particular case, another special case of the Cosserat medium model is known – the Cosserat reduced medium model, for which three of the six elastic constants, specifically $\beta, \gamma, \varepsilon$, are equal to zero and, as a consequence, there is no moment stress tensor. This model was first proposed in [42] for the description of bulk materials.

The following system of equations of dynamics is used to describe the reduced Cosserat medium [42]:

$$\begin{aligned} \rho\frac{\partial^2 \boldsymbol{u}}{\partial t^2} - (\lambda+2\mu)\,\mathrm{grad}\,\mathrm{div}\,\boldsymbol{u} + (\mu+\alpha)\,\mathrm{rot}\,\mathrm{rot}\,\boldsymbol{u} - 2\alpha\,\mathrm{rot}\,\boldsymbol{\theta} = 0, \\ I\frac{\partial^2 \boldsymbol{\theta}}{\partial t^2} - 2\alpha\,\mathrm{rot}\,\boldsymbol{\theta} + 4\alpha\boldsymbol{\theta} = 0, \end{aligned} \tag{12.5}$$

which reduces to a single vector equation in displacements

$$(\lambda+2\mu)\,\nabla\,(\nabla\cdot\boldsymbol{u})-\mu\nabla*(\nabla*\boldsymbol{u})-J\frac{\partial^2}{\partial t^2}\nabla*(\nabla*\boldsymbol{u})=\rho\frac{\partial^2\boldsymbol{u}}{\partial t^2}. \tag{12.6}$$

where the following designation ∇ is introduced in order to shorten the notation ($\nabla\cdot\boldsymbol{u}\equiv \mathrm{div}\boldsymbol{u}$, $\nabla*\boldsymbol{u}\equiv \mathrm{rot}\boldsymbol{u}$).

Let us introduce scalar φ and vector $\boldsymbol{\psi}$ potentials thus displacements vector $\boldsymbol{u}$ can be written in the following form:

$$\boldsymbol{u}=\nabla\varphi+\nabla*\boldsymbol{\psi}. \tag{12.7}$$

In the case of considering a plane problem, the vector potential will have only one component different from zero. We denote this component by ψ.

Let us substitute displacement vector (12.7) into (12.6), we obtain:

$$\nabla\left[(\lambda+2\mu)\,\Delta\varphi-\rho\frac{\partial^2\varphi}{\partial t^2}\right]+\nabla*\left[\mu\Delta\psi+J\Delta\frac{\partial^2\psi}{\partial t^2}-\rho\frac{\partial^2\psi}{\partial t^2}\right]=0. \tag{12.8}$$

Equation (12.8) is satisfied if each term of the expressions in square brackets is zero:

$$\begin{aligned}\Delta\varphi-\frac{1}{c_1^2}\frac{\partial^2\varphi}{\partial t^2}&=0,\\ \Delta\psi+G\Delta\frac{\partial^2\psi}{\partial t^2}-\frac{1}{c_2^2}\frac{\partial^2\psi}{\partial t^2}&=0.\end{aligned} \tag{12.9}$$

The following notations are introduced here: $c_1^2=\frac{(\lambda+2\mu)}{\rho}$, $c_2^2=\frac{\mu}{\rho}$, where c_1 – velocity of longitudinal wave, and c_2 - shear wave velocity in a classical medium, $G=J/\mu$.

We will seek a solution to the equations in the form of harmonic waves which propagate in the direction of the axis x and have a heterogeneous structure in z:

$$\varphi=\Phi(z)\,e^{-i(\omega t-kx)},\qquad \psi=\Psi(z)\,e^{-i(\omega t-kx)}. \tag{12.10}$$

Substituting formulas (12.10) into (12.9), we obtain from the latter ordinary differential equations:

$$\frac{\partial^2\Phi}{\partial z^2}-\nu_1^2\Phi=0,\qquad \frac{\partial^2\Psi}{\partial z^2}-\nu_2^2\Psi=0, \tag{12.11}$$

where

$$\nu_1=\left(k^2-\frac{\omega^2}{c_1^2}\right)^{\frac{1}{2}},\qquad \nu_2=\left(k^2-\frac{\omega^2}{c_2^2\left(1-G\omega^2\right)}\right)^{\frac{1}{2}}.$$

From the solutions of Eqs. (12.11) we select only those that correspond to a decrease in the wave amplitudes with depth:

$$\Phi=Ae^{-\nu_1 z},\qquad \Psi=Be^{-\nu_2 z}. \tag{12.12}$$

The postulate adopted here on the extinction of waves with depth entails the assertion that ν_α ($\alpha=1,2$) should be real and positive values, i.e. $\nu_\alpha>0$.

The final solution of equations (12.9) will have the form:

$$\varphi = Ae^{-\nu_1 z - i(\omega t - kx)}, \qquad \psi = Be^{-\nu_2 z - i(\omega t - kx)}. \tag{12.13}$$

Assuming that the boundary $z = 0$ is free of stresses, we have three conditions:

$$\sigma_{zz}|_{z=0} = 0,\ \sigma_{zx}|_{z=0} = 0,\ \sigma_{zy}\big|_{z=0} = 0. \tag{12.14}$$

In terms of displacements, these stress components are expressed as follows:

$$\sigma_{zx} = \mu\left(\frac{\partial u}{\partial z} + \frac{\partial w}{\partial x}\right) + J\left(\frac{\partial^3 w}{\partial x \partial t^2} - \frac{\partial^3 u}{\partial z \partial t^2}\right), \quad \sigma_{zz} = \lambda\left(\frac{\partial u}{\partial x} + \frac{\partial w}{\partial z}\right) + 2\mu\frac{\partial w}{\partial z}, \tag{12.15}$$

and the relation of displacements and potentials (see (12.7)) is given by the expressions:

$$u = \frac{\partial \varphi}{\partial x} - \frac{\partial \psi}{\partial z}, \qquad w = \frac{\partial \varphi}{\partial z} + \frac{\partial \psi}{\partial x}, \tag{12.16}$$

stresses can be expressed with the help of potentials in the following form:

$$\begin{aligned} \sigma_{zz} &= \lambda\left(\frac{\partial^2 \varphi}{\partial x^2} + \frac{\partial^2 \varphi}{\partial z^2}\right) + 2\mu\left(\frac{\partial^2 \varphi}{\partial z^2} + \frac{\partial^2 \psi}{\partial x \partial z}\right), \\ \sigma_{zx} &= \mu\left(2\frac{\partial^2 \varphi}{\partial x \partial z} + \frac{\partial^2 \psi}{\partial x^2} - \frac{\partial^2 \psi}{\partial z^2}\right) - J\left(\frac{\partial^4 \psi}{\partial x^2 \partial t^2} + \frac{\partial^4 \psi}{\partial z^2 \partial t^2}\right). \end{aligned} \tag{12.17}$$

Substituting expressions (12.13) into (12.17) and using boundary conditions (12.14), we obtain the following system of algebraic equations:

$$\begin{aligned} \left[\lambda\left(\nu_1^2 - k^2\right) + 2\mu\nu_1^2\right] A - 2\mu i k \nu_2 B &= 0, \\ 2\mu i k \nu_1 A + \left(\mu k^2 + \mu\nu_2^2 - J\nu_2^2\omega^2 + J\omega^2 k^2\right) B &= 0. \end{aligned} \tag{12.18}$$

From the compatibility condition of this system we obtain the relation

$$\left[\lambda\left(\nu_1^2 - k^2\right) + 2\mu\nu_1^2\right]\left[\mu\left(k^2 + \nu_2^2\right) + J\omega^2\left(k^2 - \nu_2^2\right)\right] - 4\mu\nu_1\nu_2 k^2 = 0, \tag{12.19}$$

which by introducing notations

$$\xi = \frac{c_2^2}{c_1^2} < 1,\ \eta = \frac{c^2}{c_2^2}$$

and account of dependences

$$\frac{c_1^2}{c_2^2} = \frac{\lambda + 2\mu}{\mu},\ \frac{\lambda}{\mu} = \frac{c_1^2}{c_2^2} - 2,\ \nu_1^2 = k^2 - \frac{\omega^2}{c_1^2},\ \nu_2^2 = k^2 - \frac{\omega^2}{c_2^2\left(1 - G\omega^2\right)},$$

can be transformed to the following form:

$$\eta\left[\eta^3-8\eta^2+\left(24-16\frac{\xi}{1-\frac{J}{\mu}\omega^2}\right)\eta-16\left(2-\frac{1}{1-\frac{J}{\mu}\omega^2}-\xi\right)\right]=0. \tag{12.20}$$

Note that (12.20) is a dispersion equation for calculating the phase velocity (c) of Rayleigh surface wave.

Figure 12.1 presents the dependence of the square of the phase velocity of the surface wave $\eta = c_R^2$ on frequency ω. The curves are given in dimensionless form: squared surface wave velocity c_R^2 is divided on squared shear velocity c_2^2.

The graph shows that here, in contrast to the classical case, the Rayleigh surface wave has dispersion. In the plane "phase velocity - frequency" there are two dispersion branches: the lower ("acoustic") and the upper ("optical"). As the frequency increases, the phase velocity of the wave related to the lower dispersion branch also decreases at infinity the square of the velocity of the surface wave $\eta \to 0.7$. The phase velocity of the wave related to the upper dispersion branch increases with increasing frequency. For frequencies $\omega > 9$ this growth becomes unlimited. Therefore, the upper dispersion branch describes wave processes in the frequency range $0 < \omega < 9$, further, the process ceases to be wave.

A plane shear wave is described by the second of equations (12.9):

$$\frac{\partial^2\psi}{\partial x^2}+G\frac{\partial^4\psi}{\partial x^2\partial t^2}-\frac{1}{c_2^2}\frac{\partial^2\psi}{\partial t^2}=0.$$

The solution to this equation we will look in the form:

$$\psi = Be^{i(\omega t-kx)},$$

which leads to dispersion equation

$$-k^2+Gk^2\omega^2+\frac{1}{c_2^2}\omega^2=0. \tag{12.21}$$

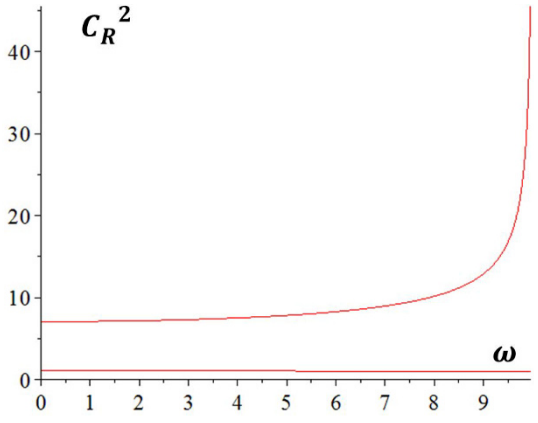

Fig. 12.1 The dependence of squared phase velocity of the surface wave on frequency

From (12.21) we determine the relationship between the frequency and the wave number of the shear wave:

$$\omega^2 = \frac{k^2 c_2^2}{1 + \frac{Gk^2}{c_2^2}}$$

and the square of the phase velocity of this wave:

$$v_{\phi\tau}^2 = \frac{\omega^2}{k^2} = \frac{c_2^2}{1 + \frac{Gk^2}{c_2^2}}.$$

Figure 12.2 presents two dependences: the square of the surface wave velocity c_R^2 (red line) and the square of the phase velocity of the shear wave v_ϕ^2 (blue line). The curves are given in dimensionless form: the square of the surface wave velocity is divided on the square of the shear wave velocity of the classical medium c_2^2, and the square of the phase velocity of the shear wave $v_{\phi\tau}^2$ is divided on c_2^2 as well. The graph shows that the phase velocity of the surface wave in the entire frequency range exceeds the phase velocity of the shear wave, which originates in unity and monotonically decreases to zero when $c_R^2 \to 0.7$, with the condition $\omega \to \infty$.

Relations (12.13) and (12.16) allow us to calculate the displacements:

$$u = (ikAe^{-\nu_1 z} + \nu_2 Be^{-\nu_2 z})\, e^{i(kx-\omega t)}, \qquad w = (-A\nu_1 e^{-\nu_1 z} + Bike^{-\nu_2 z})\, e^{i(kx-\omega t)}. \tag{12.22}$$

The constant A can be expressed through B, with the help of the second equation from (12.18):

$$B = -\frac{2i\nu_1 k\mu}{\mu k^2 + \mu\nu_2^2 - J\nu_2^2\omega^2 + Jk^2\omega^2} A,$$

then components u and w take the following form:

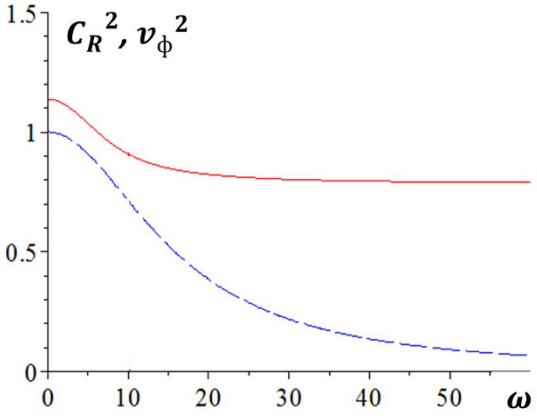

Fig. 12.2 Dependences of the squared surface wave velocity c_R^2 (red line) and the square of the phase velocity of the shear wave v_ϕ^2 (blue line) on frequency

$$u = \left(ikAe^{-\nu_1 z} - \frac{2i\nu_1 k\mu}{\mu k^2 + \mu\nu_2^2 - J\nu_2^2\omega^2 + Jk^2\omega^2} A\nu_2 e^{-\nu_2 z} \right) e^{i(kx-\omega t)},$$
$$w = \left(-A\nu_1 e^{-\nu_1 z} + \frac{2\nu_1 k^2\mu}{\mu k^2 + \mu\nu_2^2 - J\nu_2^2\omega^2 + Jk^2\omega^2} Ae^{-\nu_2 z} \right) e^{i(kx-\omega t)}. \quad (12.23)$$

Taking the real part of Eqs. (12.23), we obtain the final formulas for the displacements:

$$u = -Ak \left(e^{-\nu_1 z} - \frac{2\nu_1\nu_2\mu}{\mu k^2 + \mu\nu_2^2 - J\nu_2^2\omega^2 + Jk^2\omega^2} e^{-\nu_2 z} \right) \sin(kx - \omega t),$$
$$w = -A\nu_1 \left(e^{-\nu_1 z} - \frac{2k^2\mu}{\mu k^2 + \mu\nu_2^2 - J\nu_2^2\omega^2 + Jk^2\omega^2} e^{-\nu_2 z} \right) \cos(kx - \omega t). \quad (12.24)$$

Figure 12.3 shows the depth dependences of the displacement amplitudes u and w of the Rayleigh wave on depth in Cosserat medium and classic continuum. The curves are shown in the dimensionless form: the amplitudes of displacements are related to the amplitude of normal displacement on the surface $w|_{z=0} = 0$. Depth is shown in fractions of a wavelength.

Calculations by formulas (12.24) show that the amplitude of the displacement normal to the surface increased by about 25% compared with the classical case. The amplitude of movement parallel to the surface also increased by 90% and changed sign at depth $z = 0.18\lambda$. The graph shows that the offset parallel to the surface can exceed the transverse component in a thin near-surface layer. The trajectories of particles motion during the passage of a surface wave, as in the classical case, are ellipses.

Displacements (12.24) allow us to calculate the components of the stress tensor:

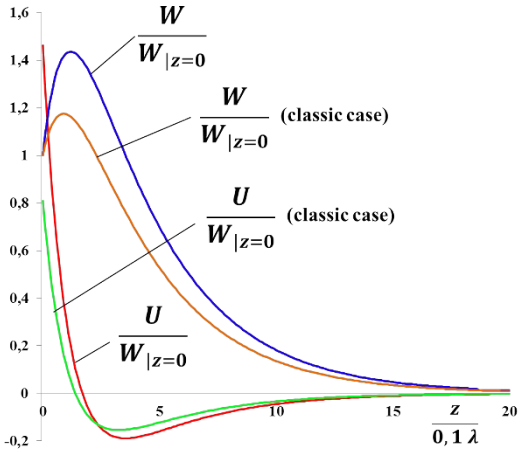

Fig. 12.3 Dependence of displacement amplitudes u and w in a Rayleigh wave on depth: amplitude of normal displacement to the surface in the simplified Cosserat model (blue line), amplitude of normal displacement to the surface in the classical model (burgundy line), amplitude of parallel displacement to the surface in the simplified Cosserat model (red line), amplitude of parallel movement to the surface in the classical model (green line).

$$\sigma_{xx} = A\left[\left(\lambda\left(\nu_1^2 - k^2\right) + 2\mu\nu_1^2\right)e^{-\nu_1 y} + \frac{4\nu_1\nu_2 k^2\mu^2}{\mu k^2 + \mu\nu_2^2 - J\nu_2^2\omega^2 + Jk^2\omega^2}e^{-\nu_2 y}\right]\cos(kx - \omega t),$$

$$\sigma_{xz} = 2A\mu\nu_1 k\left[e^{-\nu_1 y} - e^{-\nu_2 y}\right]\sin(kx - \omega t),$$

$$\sigma_{zz} = A\left[\left(\lambda\left(\nu_1^2 - k^2\right) + 2\mu\nu_1^2\right)e^{-\nu_1 y} - \frac{4\nu_1\nu_2 k^2\mu^2}{\mu k^2 + \mu\nu_2^2 - J\nu_2^2\omega^2 + Jk^2\omega^2}e^{-\nu_2 y}\right]\cos(kx - \omega t),$$

$$\sigma_{zx} = 2A\mu\nu_1 k\left[e^{-\nu_1 y} - \frac{\mu k^2 + \mu\nu_2^2 + J\nu_2^2\omega^2 - Jk^2\omega^2}{\mu k^2 + \mu\nu_2^2 - J\nu_2^2\omega^2 + Jk^2\omega^2}e^{-\nu_2 y}\right]\sin(kx - \omega t).$$

Figure 12.4 presents stress changes $\sigma_{xx}, \sigma_{xz}, \sigma_{zz}, \sigma_{zx}$ in a Rayleigh wave from the depths of half-space. The curves are presented in a dimensionless form: the stress amplitudes are related to the amplitude of the normal stress on the surface $\sigma_{xx}|_{z=0}$. The graphs also show that σ_{xx} changes sign, whereas $\sigma_{xz}, \sigma_{zz}, \sigma_{zx}$ reach a maximum at approximately $z = 1.5$ and then exponentially decreases with depth. It is also seen that the stress tensor in this case is asymmetric: the stress σ_{xz} reaches a greater value than σ_{zx}. The normal stresses in this case decrease with the depth of half-space in the same way as it does with normal stresses for the classical Rayleigh wave.

12.3 Rayleigh Waves in the Half-space of Damaged Material

Currently, the mechanics of damaged media is being intensively developed, which studies both the stress-strain state of media and the accumulation of damage in their materials. Damage is usually understood as a reduction in the elastic response of the body due to a reduction in the effective area that transfers internal forces from one part of the body to another part of it, which, in turn, is caused by the appearance

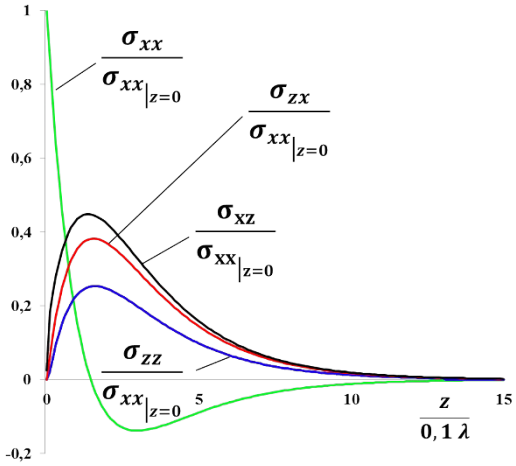

Fig. 12.4 Dependences of stress amplitudes in a surface wave on depth

and development of a scattered field of microdefects (microcracks – in elasticity, dislocations – in plasticity, micropores – in creep, surface microcracks in fatigue) [51, 52, 53].

The continuum damage mechanics has been intensively developed, starting from the fundamental works of Kachanov, generalized in [54], and Rabotnov, summarized in [55]. In traditional calculations, a measure of damage in the process of deformation development can be expressed through the scalar damage parameter $\psi(x,t)$, which characterizes the relative density of microdefects uniformly scattered per unit volume. This parameter is equal to zero when there is no damage, and is close to one at the moment of destruction.

As a rule, in the mechanics of a deformable solid, the problems of dynamics are considered separately from the problems of damage accumulation. When developing such methods, it is customary to postulate in advance that the elastic wave velocity is a given function of damage, and then experimentally determine the proportionality coefficients. The phase velocity of the wave and its attenuation are usually considered to be power functions of frequency and linear damage functions. With undoubted advantages (simplicity), this approach has a number of disadvantages, like any approach that is not based on mathematical models of processes and systems.

Let us consider a self-consistent problem with damage to the material, which includes the dynamic equation of the theory of elasticity and the kinetic equation of damage accumulation in the material of the medium. We assume that the damage is uniformly distributed in the material of the medium. Let us study the propagation of a surface wave along the free boundary of the damaged half-space. We assume that all processes are homogeneous along the third axis.

In [56, 57, 58] the problem to be self-consistent is considered, which includes, in addition to the damage development equation, the dynamic equation of elasticity theory:

$$\rho\frac{\partial^2\boldsymbol{u}}{\partial t^2}=\left(K+\frac{1}{3}G\right)\operatorname{grad}\operatorname{div}\boldsymbol{u}+G\Delta\boldsymbol{u}-\beta_1\operatorname{grad}\psi,\qquad \frac{\partial\psi}{\partial t}+\alpha\psi-\beta_2\operatorname{div}\boldsymbol{u}=0. \tag{12.25}$$

Here $\boldsymbol{u}$ – displacement vector, K – modulus of dilatation, G – shear modulus, ρ – density of the material, t – time, $\alpha=\frac{1}{\tau_*}$, β_1,β_2 – constant parameters characterizing the damage of the material and the relationship of cyclic processes with the processes of damage accumulation ($\alpha>0$); τ_* – relaxation time.

When considering the problem of the propagation of a Rayleigh surface wave in an isotropic elastic half-space in the presence of damage to its material, we restrict ourselves to the two-dimensional case when all processes are homogeneous along the axis x_2. System of Eqs. (12.25) then becomes two-dimensional and acquires the following form:

$$\rho\frac{\partial^2u_1}{\partial t^2}-(\lambda+2\mu)\frac{\partial^2u_1}{\partial x_1^2}-\mu\frac{\partial^2u_1}{\partial x_3^2}-(\lambda+\mu)\frac{\partial^2u_3}{\partial x_1\partial x_3}=-\beta_1\frac{\partial\psi}{\partial x_1}, \tag{12.26}$$

$$\rho\frac{\partial^2 u_3}{\partial t^2}-(\lambda+2\mu)\frac{\partial^2 u_3}{\partial x_3^2}-\mu\frac{\partial^2 u_3}{\partial x_1^2}-(\lambda+\mu)\frac{\partial^2 u_1}{\partial x_1\partial x_3}=-\beta_1\frac{\partial\psi}{\partial x_3}, \tag{12.27}$$

$$\frac{\partial\psi}{\partial t}+\alpha\psi=\beta_2(\lambda+2\mu)\left(\frac{\partial u_1}{\partial x_1}+\frac{\partial u_3}{\partial x_3}\right), \tag{12.28}$$

where $u_1(x_1,x_3,t)$, $u_3(x_1,x_3,t)$ – displacement vector components along the axes x_1 and x_3 respectively; λ,μ – Lamé's constants.

System of Eqs. (12.26)–(12.27) must be supplemented with boundary conditions expressing the absence of stresses on the boundary of the half-space:

$$\left[\frac{\partial u_1}{\partial x_3}+\frac{\partial u_3}{\partial x_1}\right]\Bigg|_{x_3=0}=0, \tag{12.29}$$

$$\left[\frac{\partial u_3}{\partial x_3}+\left(1-2\frac{c_\tau^2}{c_l^2}\right)\frac{\partial u_1}{\partial x_1}\right]\Bigg|_{x_3=0}=0, \tag{12.30}$$

where $c_l=\sqrt{\frac{\lambda+2\mu}{\rho}}$ and $c_\tau=\sqrt{\frac{\mu}{\rho}}$ – propagation velocities of dilation and shear waves in an infinite medium.

Eliminating the damage function from system of Eqs. (12.26)–(12.27), we obtain two equations for longitudinal and transverse displacements:

$$\begin{aligned}\frac{\partial^2 u_1}{\partial t^2}-c_l^2\left(1-\frac{\beta_1\beta_2}{\alpha}\right)\frac{\partial^2 u_1}{\partial x_1^2}-c_\tau^2\frac{\partial^2 u_1}{\partial x_3^2}-\left(c_m^2-c_l^2\frac{\beta_1\beta_2}{\alpha}\right)\frac{\partial^2 u_3}{\partial x_1\partial x_3}+\\ +\frac{1}{\alpha}\frac{\partial^3 u_1}{\partial t^3}-\frac{c_l^2}{\alpha}\frac{\partial^3 u_1}{\partial x_1^2\partial t}-\frac{c_\tau^2}{\alpha}\frac{\partial^3 u_1}{\partial x_3^2\partial t}-\frac{c_m^2}{\alpha}\frac{\partial^3 u_3}{\partial x_1\partial x_3\partial t}=0,\end{aligned} \tag{12.31}$$

$$\begin{aligned}\frac{\partial^2 u_3}{\partial t^2}-c_l^2\left(1-\frac{\beta_1\beta_2}{\alpha}\right)\frac{\partial^2 u_3}{\partial x_3^2}-c_\tau^2\frac{\partial^2 u_3}{\partial x_1^2}-\left(c_m^2-c_l^2\frac{\beta_1\beta_2}{\alpha}\right)\frac{\partial^2 u_1}{\partial x_1\partial x_3}+\\ +\frac{1}{\alpha}\frac{\partial^3 u_3}{\partial t^3}-\frac{c_l^2}{\alpha}\frac{\partial^3 u_3}{\partial x_3^2\partial t}-\frac{c_\tau^2}{\alpha}\frac{\partial^3 u_3}{\partial x_1^2\partial t}-\frac{c_m^2}{\alpha}\frac{\partial^3 u_1}{\partial x_1\partial x_3\partial t}=0,\end{aligned} \tag{12.32}$$

where $c_m=\sqrt{\frac{\lambda+\mu}{\rho}}$ $(c_\tau<c_m<c_l)$, note that $c_m^2=c_l^2-c_\tau^2$.

Consider a perturbation that propagates along the boundary $x_3=0$ and attenuates in the direction of the axis x_3. The components of the displacement vector takes the following form:

$$u_1=\frac{\partial\varphi}{\partial x_1}-\frac{\partial\theta}{\partial x_3},\qquad u_3=\frac{\partial\varphi}{\partial x_3}+\frac{\partial\theta}{\partial x_1}, \tag{12.33}$$

where φ – scalar potential ($\mathrm{rot}\,\mathrm{grad}\,\varphi=0$), θ – nonzero component of the vector potential $\boldsymbol{\theta}=\{0,\theta,0\}$ ($\mathrm{div}\,\mathrm{rot}\,\boldsymbol{\theta}=0$). The expressions for the potentials are as follows:

$$\varphi=A_1e^{-q_1x_3+i(kx_1-\omega t)},\qquad \theta=A_2e^{-q_2x_3+i(kx_1-\omega t)}, \tag{12.34}$$

where ω – frequency, k – wave number, q_1, q_2 – positive coefficients characterizing the decay of perturbations deep into the half-space, A_1, A_2 – arbitrary constants.

From system (12.29)–(12.32), taking into account (12.33)–(12.34), we find the dispersion equation

$$-c_l^2\left(k^2-q_1^2\right)\left(k^2+q_2^2\right)+2c_\tau^2k^2\left(k^2+q_2^2-2q_1q_2\right)=0, \tag{12.35}$$

in which the coefficients q_1, q_2 are defined with the following relations

$$q_1^2=k^2-\frac{(i\omega-\alpha)\,\omega^2}{(i\omega-\alpha+\beta_1\beta_2)\,c_l^2}, \qquad q_2^2=k^2-\frac{\omega^2}{c_\tau^2}. \tag{12.36}$$

From relations (12.35), (12.36) it follows that the wave number k is a complex valued $k=k_1+ik_2$. Substituting this expression into the complex dispersion equation and separating the real and imaginary parts, we obtain a system of two nonlinear algebraic equations.

In the limiting case, when there is no damage in the material, the system of algebraic equations is reduced to the dispersion equation for the Rayleigh wave, and the frequency dependence of the wave number is given by the expression

$$\omega^6-8k_1^2\omega^4+8k_1^4\left(3-2a_1^2\right)\omega^2-16k_1^6\left(1-a_1^2\right)=0 \tag{12.37}$$

where $a_1=\frac{c_\tau}{c_l}$. Dispersion equation (12.37) is written in dimensionless variables $\overline{\omega}, \overline{k}$ ($\omega=\alpha\overline{\omega}$, $k=\frac{\alpha}{c_\tau}\overline{k}$). The dimensionless propagation velocity of the Rayleigh wave is defined as $c_R=\frac{\omega}{k_1}$. It is known that the classical Rayleigh wave propagates along the free boundary of the half-space without attenuation and does not have dispersion, its velocity is a constant value for each material.

It can be seen from (12.35) and (12.36) that in the presence of damage in the material, the Rayleigh wave attenuates during propagation. Frequency dependences of the real and imaginary parts of the wavenumber for a change in the damage parameter and a fixed parameter a_1 are shown in the Figs. 12.5 and 12.6. Parameter a_1 can be expressed through Poisson coefficient (ν):

$$a_1=\sqrt{\frac{1-2\nu}{2-2\nu}}$$

and its value varies within

$$0\le a_1\le\frac{\sqrt{2}}{2}.$$

Dimensionless parameter

$$a_2=\frac{\beta_1\beta_2}{\alpha}$$

characterizes the damage of the material, the sign of this parameter depends on the signs of the initial parameters β_1, β_2, more often $a_2<0$. The dispersion curves have fundamentally different forms for positive and negative values of this parameter.

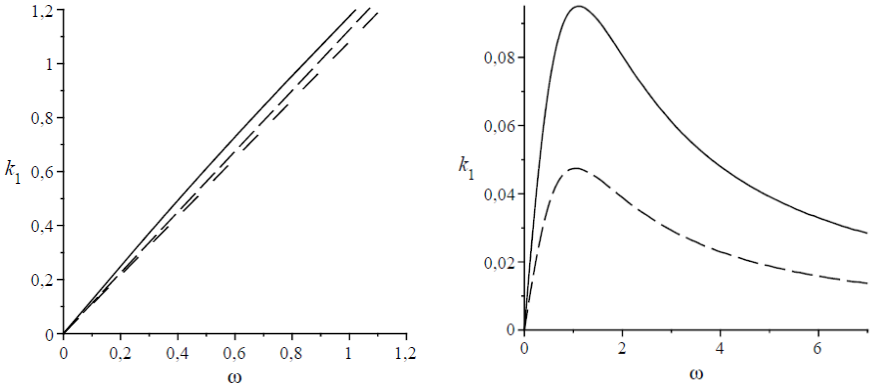

Fig. 12.5: Frequency dependences of the real part of the wave number $k_1(\omega)$ for different values of the parameter a_2: $a_2^{(1)} = -1$ (solid line), $a_2^{(2)}$ (dashed line), $a_2^{(3)} = 0$ (dashed line with spaces), $a_2^{(1)} < a_2^{(2)} < a_2^{(3)}$.

When $a_2 \neq 0$ the dispersion curves of the real and imaginary parts of the frequency have two branches, and the positive values k_1 correspond to positive values k_2, and for negative values k_1 – negative values k_2. Therefore, it is sufficient to consider these dependences in the first quarter. Figure 12.5 shows the dependences $k_1(\omega)$ for different values of the parameter a_2, here are depicted two dependences

$$f_i = k_1\left(\omega, \quad a_2 = a_2^{(i)}\right) - k_1(\omega, a_2 = 0), \qquad i = 1, 2,$$

which clearly show the existing deviations of the curve under consideration from the dispersion line corresponding to the classical Rayleigh wave.

From Figs. 12.6 and 12.7 it can be seen that the dependence $k_2(\omega)$, has a horizontal asymptote at $\omega \to +\infty$, and the damping factor $\gamma = \frac{k_2}{k_1}$ tends to zero at large values ω. When $a_2 = 0$ the graph of the dependence of the real part of the wave number on frequency is a straight line, while the imaginary part is absent.

The dependences of phase

$$v_{ph} = \frac{\omega}{k_1}$$

and group

$$v_{gr} = \frac{d\omega}{dk_1}$$

velocities on frequency are shown in Fig. 12.8. It can be seen that for a fixed non-zero value of the parameter a_2 the group velocity curve is located above the phase velocity curve; dispersion is evident at low frequencies. With a decrease in the absolute value of the damage factor, the amplitudes of both curves decrease, while the value of the phase velocity in the entire frequency range increases, and the value of the group velocity increases at lower frequencies and decreases at higher frequencies; the

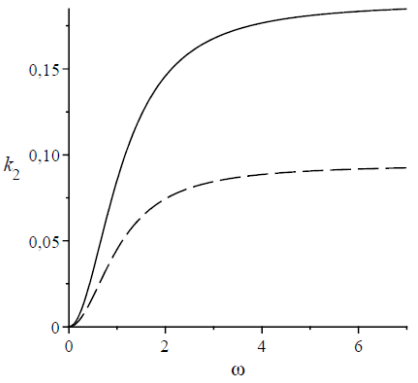

Fig. 12.6: Frequency dependences of the imaginary part of the wave number $k_2(\omega)$ for different values of the parameter a_2: $a_2^{(1)} = -1$ (solid line), $a_2^{(2)}$ (dashed line), $a_2^{(1)} < a_2^{(2)} < 0$.

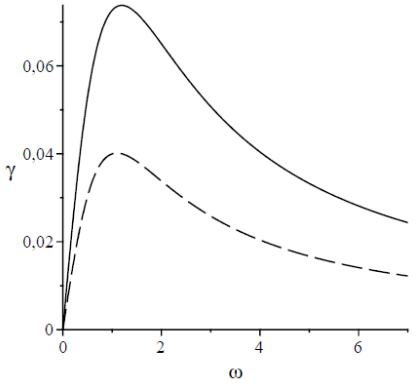

Fig. 12.7: Attenuation coefficient dependences $\gamma(\omega)$ for different values of the parameter a_2: $a_2^{(1)} = -1$ (solid line), $a_2^{(2)}$ (dashed line), $a_2^{(1)} < a_2^{(2)} < 0$.

Fig. 12.8 Dependences of phase $v_{ph}(\omega)$ (1) and group velocities $v_{gr}(\omega)$ (2) velocities at different values of the parameter a_2: $a_2^{(1)} = -1$ (solid line), $a_2^{(2)}$ (dashed line), $a_2^{(3)} = 0$ (dashed line with spaces), $a_2^{(1)} < a_2^{(2)} < a_2^{(3)}$

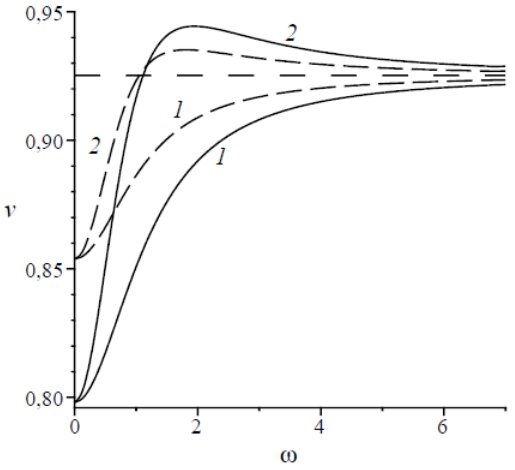

maximum of the group velocity function drops and shifts towards low frequencies. When $a_2 = 0$ curves of phase and group velocities coincide $v_{ph} = v_{gr} = \text{const}$, where the constant is given by equation (12.37) and depends only on Poisson coefficient.

12.4 Conclusion

We consider a simplified (reduced) dynamic model of a Cosserat medium, which occupies an intermediate position between the classical dynamic theory of elasticity

and the proper Cosserat medium model, which has asymmetry in the stress tensor and the presence of moment stresses. In contrast to the latter, in the simplified model, three of the six elastic constants are zero and, as a result, there is no moment stress tensor.

In the two-dimensional formulation for the model of a reduced medium, the problem of the propagation of an elastic surface wave along the half-space boundary was solved. The solution of the equations was described as the sum of the scalar and vector potentials, and only one component of the vector potential is nonzero. It is shown that such a wave, in contrast to the classical surface Rayleigh wave, has a dispersion. The phase velocity of the surface wave in the entire frequency range exceeds the phase velocity of the bulk shear wave. The stresses and displacements arising in the zone of propagation of the surface wave are calculated.

In the presence of damage in the medium, surface waves attenuate in the process of propagation along the boundary of the half-space and have dispersion. The presence of damage contributes to the appearance of insignificant dispersion in the low-frequency range. The smaller the value of the damage coefficient, the less its manifestation. The dispersion is anomalous. In the absence of damage in the medium, the surface wave propagates without dispersion and attenuation.

Acknowledgements The work was supported by Russian Science Foundation (project 20-19-00613).

References

[1] Lord Rayleigh (1985) On waves propagated along the plane surface of an elastic solid, Proceedings of the London Mathematical Society **S1-17**(1):4-11. DOI 10.1112/plms/s1-17.1.4

[2] Aki K, Richards PG (2002) Quantitative Seismology: Theory and Methods, 2nd ed, New York, Freeman, University Science Books.

[3] Krylov VV (1994) On the theory of railway-induced ground vibrations, Journal de Physique IV Proceedings **4**(C5):769-772. DOI 10.1051/jp4:19945167

[4] Krylov VV, Ferguson CC (1994) Calculation of low-frequency ground vibrations from railway trains, Applied Acoustics **42**:199-213. DOI 10.1016/0003-682X(94)90109-0

[5] Krylov VV (1995) Generation of ground vibrations by superfast trains, Applied Acoustics. **44**:49-164. DOI 10.1016/0003-682X(95)91370-I

[6] Krylov VV (1996) Vibrational impact of high-speed trains. I. Effect of track dynamics, Journal of the Acoustical Society of America **101**(6):3121-3134. DOI 10.1121/1.417123

[7] Krylov VV (1997) Spectra of low-frequency ground vibrations generated by high-speed trains on layered ground, Journal of Low Frequency Noise, Vibration and Active Control **16**(4):257-270. DOI 10.1177/026309239701600404

[8] Krylov VV (1998) Effect of track properties on ground vibrations generated by high-speed trains. Acustica united with Acta Acustica **84**(1):78-90.
[9] Krylov VV (1999) Ground vibration boom from high-speed trains, Journal of Low Frequency Noise, Vibration and Active Control **18**(4):207-218. DOI 10.1177/026309239901800405
[10] Krylov VV (Ed) (2001) Noise and Vibration from High Speed Trains, London, Thomas Telford Publishing.
[11] Vesnitsky AI (2001) Waves in Systems with Moving Boundaries and Loadings (in Russ), Moscow, Fizmatlit.
[12] Denisov GG, Novikov VV, Kugusheva EK (1985) On the problem of the stability of one-dimensional unbounded elastic systems, Journal Applied Mathematics and Mechanics **49**(4):533-537. DOI 10.1016/0021-8928(85)90065-6
[13] Butova SV, Gerasimov SI, Erofeev VI, Kamchatnyi VG (2015) Stability of high-speed objects moving along a rocket track guide, J Mach Manuf Reliab **44**:1-5. DOI 10.3103/S1052618815010021
[14] Gerasimov SI, Erofeev VI (2016) Calculation of flexural-and-torsional vibrations of a rocket track rail, J Mach Manuf Reliab **45**:211-213. DOI 10.3103/S1052618816030055
[15] Gerasimov SI, Erofeev VI, Kamchatnyi VG, Odzerikho IA (2018) The sliding contact condition in stability analysis of stage motion for a rocket sled track facility, J Mach Manuf Reliab **47**:221-226. DOI 10.3103/S105261881803007X
[16] Ermolov IN, Lange YV (2004) Ultrasound Control (in Russ), vol 3 of Kluev VV (Ed) Nondestructive Testing: a Guide in 7 Volumes, Moscow, Mashinostroenie.
[17] Gulyaev YV (2005) Acoustoelectronics (historical review), Physics – Uspekhi **48**:847-855. DOI 10.1070/PU2005v048n08ABEH002840
[18] Maugin GA, Metrikine AV (Eds) (2010) Mechanics of Generalized Continua: on Hundred Years after the Cosserats, Advanced in Mathematics and Mechanics, vol 21, Springer, Berlin. DOI 10.1007/978-1-4419-5695-8
[19] Altenbach H, Maugin GA, Erofeev V (Eds) Mechanics of Generalized Continua, Advanced Structured Matherials, vol 7, Springer, Berlin-Heidelberg. DOI 10.1007/978-3-642-19219-7
[20] Altenbach H, Forest S, Krivtsov A (Eds) (2013) Generalized Continua as Models with Multi-Scale Effects or Under Multi-Field Actions, Advanced Structured Matherials, vol 22, Springer, Berlin-Heidelberg. DOI 10.1007/978-3-642-36394-8
[21] Altenbach H, Eremeyev VA (Eds) (2013) Generalized Continua – from the Theory to Engineering Applications, CISM International Centre for Mechanical Sciences, vol 541,Springer, Wien. DOI 10.1007/978-3-7091-1371-4
[22] Bagdoev AG, Erofeyev VI, Shekoyan AV (2016) Wave Dynamics of Generalized Continua, Advanced Structured Materials, vol 24, Springer, Berlin-Heidelberg. DOI 10.1007/978-3-642-37267-4
[23] Altenbach H, Forest S (Eds) (2016) Generalized Continua as Models for Classical and Advanced Materials, Advanced Structured Matherials vol 42, Springer, Berlin-Heidelberg. DOI 10.1007/978-3-319-31721-2

[24] Maugin GA. (2017) Non-Classical Continuum Mechanics, Advanced Structured Matherials, vol 51, Springer, Singapore. DOI 10.1007/978-981-10-2434-4
[25] dell'Isola F, Eremeyev VA, Porubov A (2018) Advanced in Mechanics of Microstructured Media and Structures, Advanced Structured Matherials, vol 87, Springer, Cham. DOI 10.1007/978-3-319-73694-5
[26] Altenbach H, Pouget J, Rousseau M, Collet B, Michelitsch T (2018) Generalized Models and Non-Classical Approaches in Complex Materials 2, Advanced Structured Matherials, vol 89, Springer, Cham. https://doi.org/10.1007/978-3-319-72440-9
[27] Altenbach H, Pouget J, Rousseau M, Collet B, Michelitsch T (2018) Generalized Models and Non-Classical Approaches in Complex Materials 2, Advanced Structured Matherials, vol 90, Springer, Cham. DOI 10.1007/978-3-319-77504-3
[28] Erofeev V, Porubov A, Sargsyan S (2018) Materials Physics and Mechanics **35** (Nonlinear Wave Dynamics of Generalized Continua, Special issue dedicated to the memory EL Aero and GA Maugin).
[29] Altenbach H, Belyaev A, Eremeyev V (Eds) (2019) Dynamical Processes in Generalized Continua and Structures, Advanced Structured Matherials, vol 103, Springer, Cham. DOI 10.1007/978-3-030-11665-1
[30] Sumbatyan MA (Ed) (2019) Wave Dynamics, Mechanics and Physics of Microstructured Metamaterials, Advanced Structured Matherials, vol 109, Springer, Cham. DOI 10.1007/978-3-030-17470-5
[31] Altenbach H, Müller WH, Abali BE (Eds) (2019) Higher Gradient Matherials and Related Generalized Continua, Advanced Structured Matherials, vol 120, Springer, Cham, DOI 10.1007/978-3-030-30406-5
[32] Erofeev VI, Pavlov IS (2019) Structural Modeling of Metamaterials, Advanced Structured Matherials, vol 144, Springer, Cham. DOI 10.1007/978-3-030-60330-4
[33] Lur'ye SA (2020) On the paradox of anomalous relative bending stiffness of ultrathin beams in the gradient theory of elasticity, Mech Solids **55**(3):340-347. DOI 10.3103/S0025654420030085
[34] Eremeev V.A, Lebedev LP (2020) On solvability of boundary value problems for elastic micropolar shells with rigid inclusions, Mech Solids **55**:852-856. DOI 10.3103/S0025654420050052
[35] Radaev YN (2020) Factorization of the main hyperbolic differential operator of the micropolar elasticity theory, Mech Solids **55**:776-783. DOI 10.3103/S0025654420060126
[36] Tarlakovskii DV, Nguyen VL (2021) Estimation of taking into account the moment properties of the medium on the example of a nonstationary axisymmetric problem, Mech Solids **56**:1013-1019. DOI 10.3103/S0025654421060182
[37] Murashkin EV, Radaev YN (2021) Generalization of the algebraic Hamilton – Cayley theory, Mech Solids **56**:996-1003. DOI 10.3103/S0025654421060145
[38] Vasil'ev VV, Lurie SA, Salov VA (2021) New solution to the problem of a crack in an orthotropic plate under tension, Mech Solids **56**:902-910. DOI 10.3103/S0025654421060200

[39] Murashkin EV, Radaev YN (2022) On theory of oriented rensor elements of area for a micropolar continuum immersed in an external plane space, Mech Solids **57**:205-213. DOI 10.3103/S0025654422020108
[40] Cosserat E, Cosserat F (1909) Theorie des Corps Deformables, Paris: Librairie Scientifique A Hermann et Fils. DOI 10.1038/081067a0
[41] Nowacki W (1986) Theory of Asymmetric Elasticity, Pergamon Press.
[42] Schwartz LM, Jonson DL, Feng S (1984) Vibrational models in granular materials, Physical Review Letters **52**(10):831-834. DOI doi.org/10.1103/PhysRevLett.52.831
[43] Grekova EF (2016) Plane waves in the linear elastic reduced Cosserat medium with a finite axially symmetric coupling between volumetric and rotational strains, Math Mech Solids **21**(1):73-93. DOI 10.1177/1081286515577042
[44] Grekova EF (2018) Waves in elastic reduced Cosserat medium with anisotropy in the term coupling rotational and translational strains or in the dynamic term, In: dell'Isola F, Eremeyev VA, Porubov A (Eds) Advances in Mechanics of Microstructured Media and Structures, Advanced Structured Materials, vol. 87, pp 143-156, Springer, Cham. DOI 10.1007/978-3-319-73694-5_9
[45] Grekova EF (2019) Reduced enhanced elastic continua as acoustic metamaterials, In: Altenbach H, Belyaev A, Eremeyev VA, Krivtsov A, Porubov AV (Eds) Dynamical Processes in Generalized Continua and Structures, Advanced Structured Materials, vol 103, pp 253-268, Springer, Cham. DOI 10.1007/978-3-030-11665-1_14
[46] Le Roux J (1911) Étude géométrique de la torsion et de la flexion dans la déformation infinitésimale d'un milieu continu, Annales scientifiques de l'ÉNS, 3e série **28**:523-579. DOI 10.24033/asens.643
[47] Le Roux J (1913) Recherches sur la géométrie des déformations finies, Annales scientifiques de l'ÉNS, 3e série **30**:193-245. DOI 10.24033/asens.659
[48] Jaramillo TJ (1929) A Generalization of the Energy Function of Elasticity Theory, PhD Dissertation, Chicago, University of Chicago.
[49] Erofeyev VI (2003) Wave Processes in Solids with Microstructure, World Scientific Publishing, New Jersey et al.
[50] Antonov AM, Erofeev VI (2018) Rayleigh wave on the boundary of gradient-elastic semi-space (in Russ), Herald of the Bauman Moscow State Tech Univ, Nat Sci (4):59-72. DOI 10.18698/1812-3368-2018-4-59-72
[51] Maugin GA (1992) The Thermomechanics of Plasticity and Fracture, Cambridge University Press.
[52] Lemaitre J (1992) A Course on Damage Mechanics, Springer, Berlin.
[53] Krajcinovic D (1996) Damage Mechanics, Elsevier Science, Amsterdam.
[54] Kachanov LM (1986) Introduction to Continuum Damage Mechanics, Springer, New York.
[55] Rabotnov YN (1969) Creep Problems in Structural Members, North-Holland Series in Applied Mathematics and Mechanics, North-Holland Publishing Company, Amsterdam.

[56] Erofeev VI, Nikitina EA (2010) The self-consistent dynamic problem of estimating the damage of a material by an acoustic method, Acoustical Physics **56**(4):584-587. DOI 10.1134/S106377101004024X

[57] Erofeev VI, Nikitina EA, Sharabanova AV (2010) Wave propagation in damaged materials using a new generalized continuum, In: Maugin GA, Metrikine AV (Eds) Mechanics of Generalized Continua. One Hundred Years After the Cosserats, Advances in Mechanics and Mathematics, vol 21, Springer, Heidelberg, pp 143–148. DOI doi10.1007/978-1-4419-5695-8_15

[58] Stulov A, Erofeev V (2016) Frequency-dependent attenuation and phase velocity dispersion of an acoustic wave propagating in the media with damages, In: Altenbach H, Forest S (Eds) Generalized Continua as Models for Classical and Advanced Materials, Advances Structured Materials, vol 42, Springer, Cham, pp 413–423. DOI 10.1007/978-3-319-31721-2_19